Available online at www.sciencedirect.com
SCIENCE DIRECT®
Journal of Power Sources 146 (2005) 300–303
JOURNAL OF POWER SOURCES
www.elsevier.com/locate/jpowsour

Cathode properties of birnessite type manganese oxide prepared by using vanadium xerogel

Y. Matsuo*, Y. Miyamoto, T. Fukutsuka, Y. Sugie

Graduate School of Engineering, University of Hyogo, 2167 Shosha, Himeji, Hyogo 671-2201, Japan

Abstract

Birnessite type manganese dioxides containing a small amount of vanadium were synthesized by oxidizing manganese nitrate with vanadium xerogel and hydrogen peroxide in a basic solution. When the nominal manganese/vanadium molar ratio was between 0.25 and 1, the resulting samples possessed birnessite type structure with irregular stacking of manganese dioxide layers, otherwise the products became amorphous. The obtained birnessite type manganese dioxides had a characteristic sponge-like and open-network microstructure composed of interconnected bent layer and the particle size was very small, less than 1 μm. The discharge capacity at the second cycle became maxima and reached 250 mAh g^{-1} for the sample prepared with the nominal Mn/V ratio of 1 and the cycling property was relatively good. The increase of utilization of active material due to the increase of electrical conductivity as the result of introduction of vanadium and/or the characteristic microstructure would lead the high discharge capacity. The irregular stacking of manganese oxide layers would be responsible for the relatively good cycling behavior.

Keywords: Birnessite; Manganese oxide; Vanadium xerogel

1. Introduction

Birnessite type manganese dioxide is one of the interesting cathode active materials of lithium rechargeable batteries. It has been reported that birnessite has a large discharge capacity in the 3 V region; however, the cycling performance was inadequate because of the conversion of layered structure to the more stable spinel during electrochemical insertion/extraction of lithium ions [1–3]. Recently, the cycling performance of birnessite was improved by stabilizing the layer structure using bismuth [2], vanadate [4] or magnesium [5] ions as pillar and by partially substituting manganese in the layer of sodium birnessite by cobalt [6]. The incorporation of cobalt into the layer of birnessite by substituting manganese not only stabilizes the layer structure but also increase the conductivity of birnessite [7], probably leading the increase of utilization of active material. Composite electrode with carbon black obtained by coprecipitation technique also enhanced the utilization of active material [8]. Very recently, Wang et al. reported that cycling performance was improved for the disordered birnessite prepared from exfoliated MnO_2 nanosheets [9]. They suggested that the irregular layer-to-layer registry might provide a high-energy barrier against phase conversion toward spinel structure.

Preparation of the birnessite type manganese oxide has been performed in several ways, including a simple redox sol–gel reaction starting from permanganate [10], calcination [11] and hydrothermal reaction [12] of permanganate and oxidation of manganese nitrate by hydrogen peroxide or manganese hydroxide, oxygen [7,13,14], chlorine [13] and permanganate [3] in an alkaline solutions.

In this study, birnessite type manganese oxide containing a small amount of vanadium was prepared by using vanadium xerogel and hydrogen peroxide as oxidizing reagents in a basic solution, and the cathode properties of the obtained samples were investigated.

2. Experimental

Birnessite type manganese oxide was prepared based on the method employed for the synthesis of manganese

---

* Corresponding author.
E-mail address: ymatsuo@eng.u-hyogo.ac.jp (Y. Matsuo).

0378-7753/$ – see front matter © 2005 Published by Elsevier B.V.
doi:10.1016/j.jpowsour.2005.03.111

oxide/graphite oxide nanocomposite which was reported by Yang et al. [15] except the use of vanadium xerogel in stead of graphite oxide. Vanadium xerogel was prepared according to the report by Lemerle et al. [16]. Polyvanadic acid was prepared by the spontaneous polymerization of decavanadic acid, which was obtained by dropping aqueous solution of sodium metavanadate on an ion exchange resin (DOWEX 50W-X2, 50–100 mesh, H-form) bed. The resulting solution was allowed to stand until the solvent evaporated at room temperature and vanadium xerogel was formed. The yellow aqueous solution of lithium hydroxide (0.15 M, 4 ml) containing vanadium xerogel (100 mg) was mixed with hydrogen peroxide (30%, 21 ml), manganese nitrate aqueous solution (0.3 M, 0.95–7.6 ml; nominal Mn/V ratio of 0.25–2), lithium hydroxide solution (0.5 M, 6.4 ml) and then hydrogen peroxide (30%, 6 ml). The dark brown precipitate was centrifuged, filtrated, washed with water and then dried at 60 °C. The obtained samples were analyzed by X-ray diffraction (Rigaku Rint-2100), FT-IR (Nicolet Avatar 360), SEM (JEOL JSM-5600), TG/DTA (Shimadzu TG50) measurements and elemental analysis by X-ray fluorescence measurement (Seiko Instruments, SEA 2001). TG/DTA measurement was carried out between room temperature and 500 °C with a temperature increase rate of 10 °C min^{-1}. The mean oxidation number of the samples was determined with iodemetric titration method. For electrochemical study, the samples were mixed with conducting acetylene black and PVdF as binder (70:20:10, w/w/w) and then sandwiched by Ni mesh. This was pressed at 500 kg cm^{-2} under vacuum and dried at 120 °C overnight. Pure lithium metal was counter and reference electrode. A propylene carbonate containing 1 M of $LiClO_4$ (Kishida Chemical) was used as an electrolyte solution. Charge–discharge measurement was performed at a C/24 rate between 2 and 4 V versus Li/Li^+ under Ar atmosphere. Both charge and discharge started just after the potential reached cut-off voltage.

3. Results and discussion

3.1. Preparation of birnessite type manganese dioxides

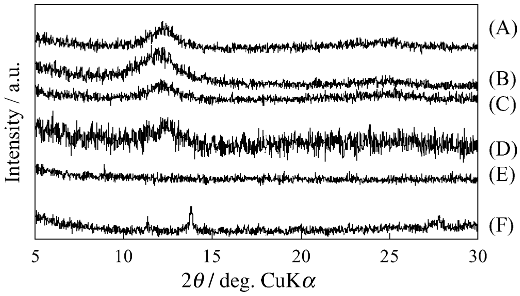

Fig. 1. X-ray diffraction patterns of manganese oxides prepared with various Mn/V ratios: (A) 0.25, (B) 0.5, (C) 0.75, (D) 1, (E) 1.5 and (F) 2.

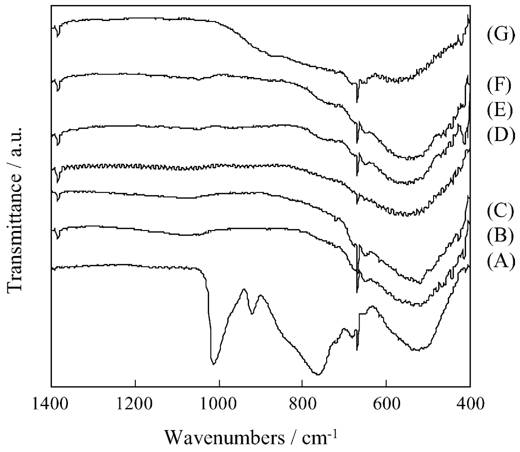

Fig. 2. IR spectra of vanadium xerogel (A) and manganese oxide prepared with various Mn/V ratios: (B) 0.25, (C) 0.5, (D) 0.75, (E) 1, (F) 1.5 and (G) 2.

Fig. 1 shows the X-ray diffraction patterns of the obtained samples with various nominal manganese nitrate/vanadium xerogel ratios. A broad diffraction peak at $2\theta = 11.8^\circ$ was observed for the samples with Mn/V ratio of less than 1, while no diffraction peak was observed for the samples with Mn/V ratio larger than 1.The *d*-spacing calculated from this peak was 0.75 nm which was much smaller than the interlayer spacing of vanadium xerogel (1.17 nm) and dehydrated vanadium xerogel (0.88 nm) [17] and was similar to that of hydrated birnessite type manganese oxide (0.71 nm). X-ray fluorescence measurement indicated that the vanadium contents were less than 8% of that of manganese for the samples with Mn/V ratios less than 1. Fig. 2 shows the IR spectra of vanadium xerogel and the sample with various Mn/V ratios. The absorption peaks at 1010 and 750 cm^{-1} due to V=O and terminal V–O disappeared and a broad peak at 540 cm^{-1} was observed, which could be due to lattice vibration of manganese oxide [10]. These suggest that the obtained samples were mainly consisting of manganese oxide, probably with a birnessite type structure.

Fig. 3 shows the X-ray diffraction patterns of the samples prepared without hydrogen peroxide or vanadium xerogel with a nominal Mn/V ratio of 1. In the absence of hydrogen peroxide, the vanadium/manganese ratio in the sample determined by X-ray fluorescence measurement was 1.6, which

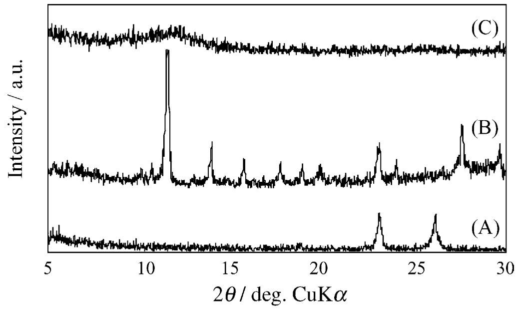

Fig. 3. X-ray diffraction patterns of the products prepared without (A) hydrogen peroxide and (B) vanadium xerogel, together with that of (C) manganese oxide prepared with nominal Mn/V ratio of 1.

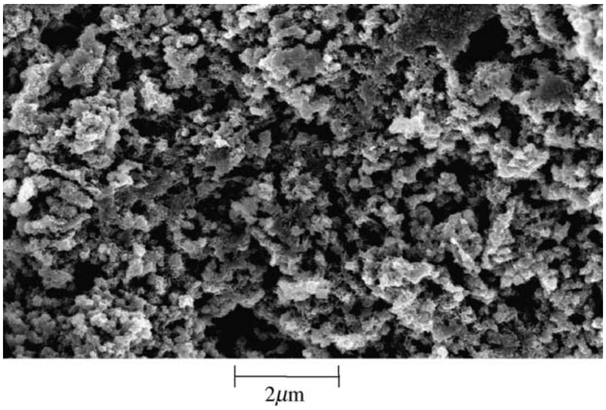

Fig. 4. SEM image of manganese oxide prepared with nominal Mn/V ratio of 1.

was much higher than that observed for the sample obtained in the presence of hydrogen peroxide and a lot of peaks which were not attributed to known manganese oxides or vanadium oxides were observed (Fig. 3(B)). This would be because the reduced form of vanadium xerogel as the result of oxidation of manganese nitrate precipitated together with the oxidized manganese, providing a complicated product. However, in the presence of hydrogen peroxide, the reduced form of vanadium xerogel would be readily reoxidized before precipitation, forming water soluble vanadium xerogel again and this was removed from the sample during washing it with water. On the other hand, in the absence of vanadium xerogel, as shown in Fig. 3(A), two diffraction peaks at $2\theta = 23.5^\circ$ and 26.5°, instead of 11.8° were observed, which indicates that the product does not possess layered structure. This suggests that in order to construct the layer structure of manganese oxide, layered vanadium xerogel is inevitable in the present system.

Fig. 4 shows the SEM image of the sample with Mn/V ratio of 1. The particle size was very small (less than 1 μm) and these had a characteristic sponge-like and open-network microstructure composed of interconnected bent layers, which was similar to that of vanadium oxide reported by Torardi et al. [18]. The manganese oxide nanosheets formed on vanadium xerogel would be interconnected during oxidation process and these nanosheets were stacked irregularly, providing the above unique morphology. In an X-ray diffraction pattern of the sample prepared with a nominal Mn/V ratio of 1, broad (1 0) and (1 1) bands at $2\theta = 36.7^\circ$ and 65.8° were observed, respectively, and general ($h\,k\,l$) diffraction was absent, which indicates poor sheet-stacking sequence [9,19].

The samples showed a monotonic weight loss up to 200 °C, which would be due to desorption of surface water and removal of interlayer water. The loss due to water was 10–14%, which was rather high when compared with, those observed for birnessites [11] and comparable to Mg- or Zn-birnessites reported by Aronson et al. [2,5,11]. Table 1 shows the content of water, together with mean oxidation number and vanadium/manganese ratio. Mean oxidation number was calculated assuming that the samples contained only manganese. It was almost four especially for the samples with low nominal Mn/V ratios, probably because of the contribution of residual vanadium xerogel with a high valence of vanadium. As the nominal Mn/V ratio increases, vanadium with lower valences formed, as the result of oxidation of Mn^{2+} ion would be included into the product, reducing the mean oxidation number of the sample.

Table 1
Mn/V ratio, content of lattice water and mean oxidation number of manganese oxide with various nominal Mn/V ratios

Nominal Mn/V ratio	Mn/V ratio	Content of lattice water (%)	Mean oxidation number[a]
0.25	0.03	14.4	4.01
0.5	0.03	14.1	3.92
0.75	0.03	13.3	3.80
1.0	0.05	12.3	3.70
1.25	0.08	14.4	3.88
2.0	0.32	10.7	–

[a] Mean oxidation number was determined based on iodmetric titration, assuming that the samples contain only manganese.

3.2. Charge–discharge properties of birnessite type manganese dioxides

Fig. 5 shows the charge–discharge curves of the sample prepared with nominal Mn/V ratio of 1. It showed a large capacity around 2.7 V, which is typical for birnessite type manganese oxide and the first and second discharge capacity reached 239 and 252 mAh g^{-1}, respectively. These values were higher than or comparable to those reported for birnessite type manganese oxides modified by Mg^{2+} [5] or Co [6]. The discharge capacity at the 10th cycle was still 199 mAh g^{-1}, indicating relatively good cycling behavior.

Tsuda et al. prepared birnessite type manganese oxide partially substituted cobalt and observed the considerable increase of discharge capacity, though the doped cobalt was electrochemically inactive. They also suggested that the increase of electrical conductivity would increase the utilization of active material. Additives such as carbon black [8] or Nafion [20] to birnessite improved cyclability and increased the utilization of active material even at a high rate because of the enhanced electrical or ionic conductivity. The effect of

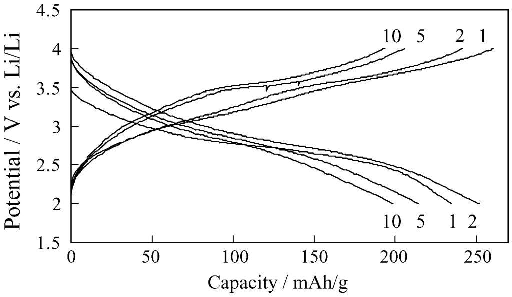

Fig. 5. Charge–discharge curves of manganese oxide prepared with nominal Mn/V ratio of 1.

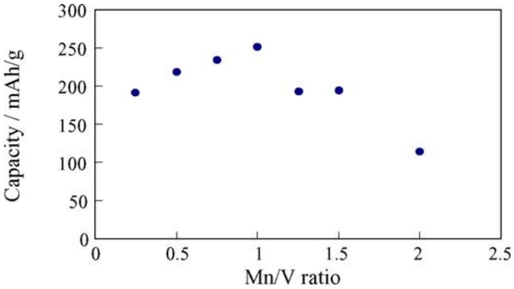

Fig. 6. Relationship between second discharge capacity and nominal Mn/V ratios.

vanadium in the present sample is not clear at this moment; however, it may increase the conductivity of the samples if they are introduced in the skeleton of the birnessite layer. On the other hand, Torardi indicated that the characteristic morphology of vanadium xerogel similar to that observed in this study was favorable for the lithium transport and this lead the increase of utilization of active material [18]. These facts suggest that morphology and structural effects would be mainly responsible for the large discharge capacity of birnessite containing a small amount of vanadium obtained in this study. In addition to these, the irregular layer-to-layer registry of birnessite prepared from exfoliated MnO_2 nanosheets has been suggested to improve cyclability because of a high-energy barrier against phase conversion toward spinel structure [9]. The irregular stacking of manganese oxide layers would be responsible for the relatively good cycling behavior of the present samples.

The discharge curves of manganese oxides with various nominal Mn/V ratios were similar to that of the sample with Mn/V = 1, showing a considerable capacity around 2.7 V. The discharge capacity of the samples prepared with various Mn/V ratios as a function of nominal Mn/V ratio is shown in Fig. 6. The discharge capacity increased until the Mn/V ratio became unity and then decreased. As shown in Fig. 1 and Table 1, various parameters such as structure, composition and properties of the samples which might affect the charge–discharge property changed in a complicated manner; therefore, it is very difficult to know the reason why the sample with Mn/V = 1 showed the maximum discharge capacity. However, it appears that the sample with layered structure and lower water content and appropriate vanadium content would be favorable.

Acknowledgement

Financial support from Nichirin Co. Ltd. is greatly acknowledged.

References

[1] P. Strobel, C. Moget, Mater. Res. Bull. 28 (1993) 93.
[2] S. Bach, J.-P. Pereira-Ramos, C. Cachet, M. Bode, L.T. Yu, Electrochim. Acta 40 (1995) 785.
[3] S. Bach, J. Pereira-Ramos, N. Baffier, J. Electrochem. Soc. 143 (1996) 3492.
[4] F. Zhang, K. Ngala, M.S. Whittingham, Electrochem. Commun. 2 (2000) 445.
[5] B.J. Aronson, A.K. Kinser, S. Passerini, W.H. Smyl, A. Stein, Chem. Mater. 11 (1999) 949.
[6] M. Tsuda, H. Arai, Y. Sakurai, J. Power Sources 110 (2002) 52.
[7] P.K. Sharma, G.J. Moore, F. Zhang, P. Zavalij, M.S. Wittingham, Electrochem. Solid State Lett. 2 (1999) 494.
[8] X. Yang, W. Tang, Z. Liu, Y. Makita, S. Kasaishi, K. Ooi, Electrochem. Solid State Lett. 5 (2002) 191 (LiBir).
[9] L. Wang, K. Takada, A. Kajiyama, M. Onoda, Y. Miyake, L. Zhang, M. Watanabe, T. Sasaki, Mater. Chem. 15 (2003) 4508.
[10] R. Renuka, S. Ramamurthy, J. Power Sources 87 (2000) 144 (IR).
[11] S. Komaba, N. Kumagai, S. Chiba, Electrochim. Acta 46 (2000) 31.
[12] R. Chen, M.S. Whittingham, J. Electrochem. Soc. 144 (1997) L64.
[13] Q. Feng, E.-H. Sun, K. Yanagisawa, N. Yamazaki, J. Ceram. Soc. Jpn. 105 (1997) 564.
[14] C. Julien, M. Massot, R. Baddour-Hadjean, S. Franger, S. Bach, J. Pereira-Ramos, Solid State Ionics 159 (2003) 345.
[15] X. Yang, Y. Makita, Z.-H. Liu, K. Ooi, Chem. Mater. 15 (2003) 1228.
[16] J. Lemerle, L. Nejem, J. Lefebure, J. Inorg. Nucl. Chem. 42 (1980) 17.
[17] P. Aldebert, N. Baffier, N. Gharbi, J. Livage, Mater. Res. Bull. 16 (1981) 669.
[18] C.C. Torardi, C.R. Miao, M.E. Lewittes, Z. Li, J. Solid State Chem. 163 (2002) 93.
[19] T. Sasaki, S. Nakano, S. Yamauchi, M. Watanabe, Chem. Mater. 9 (1997) 602.
[20] X. Yang, W. Tang, Z.-H. Liu, K. Ikeda, K. Ooi, Chem. Lett. 32 (2003) 1160.